

Fundamentals and Applications of Liquid Crystal-Based, Polarization-Dependent Diffractive Optics

**Hiroyuki Yoshida, SeongYong Cho, Yuto Tsuboi,
Yuji Tsukamoto, and Masanori Ozaki**

Division of Electrical, Electronic, and Information Engineering, Osaka University,
2-1 Yamadaoka, Suita, Osaka 565-0871 JAPAN
Keywords: Diffractive Optics, Holography, Photoalignment

ABSTRACT

There is recently interest in LC-based diffractive optical elements (DOEs) that enable modulation of the light phasefront through the spatial distribution of its optic axis. The operating principles of both transmissive and reflective devices are reviewed and their applications are discussed.

1 INTRODUCTION

Conventional optical systems guide light using bulky elements such as lenses and mirrors, but the spread of wearable devices is pushing the need for miniature optical elements that can control light. Diffractive optical elements (DOEs) in which light transmission or reflection characteristics is determined by the structural design is becoming more common in optical systems. Recent advances in nanofabrication techniques are opening new frontiers in diffractive devices, as they enable multiple optical functions to be integrated in a single device, based on the metasurface concept [1].

LC materials with self-organized birefringent structures, on the other hand, enable fabrication of DOEs fabricated without the need of complex nano-fabrication methods. Their operation is based on the Pancharatnam-Berry phase or geometric phase, in which light propagating through the device acquires a phase that is proportional to twice the azimuthal orientation of the optic axis [2]. By using the nematic and chiral LC phases, both transmissive (standard DOE) and reflective devices (also known as holographic optical elements, or HOEs) are achievable [3,4]. Among the various platforms available for DOEs, LCs are one of the most attractive, as established methods exist to control their optic axis orientation, and they have negligible absorption, leading to high diffraction efficiencies. By employing polymerizable LC materials, devices as large as 75 mm have been fabricated by a simple coating process [5]. A see-through-type near-eye display prototype based on a LC HOEs has been recently achieved [6].

Here, we first review the operating principle of transmissive and reflective DOEs based on LCs. Further, we show that HOEs based on chiral LCs possess unique properties that make them distinct from competing technologies.

2 PRINCIPLE OF PHASE MODULATION USING PATTERNED NEMATIC LCS

A nematic LC (NLC) layer with half-wave retardation imparts a phase on circularly polarized light that is proportional to twice the azimuthal orientation of the optic axis; this phase is known as the Pancharatnam-Berry or geometric phase. Its operation mechanism can be described using Jones calculus as follows (note that the $e^{i(\omega t - kz)}$ convention is employed to describe light propagation along the z-axis). The Jones matrix of a uniaxial plate with phase retardation Δ and slow axis at an angle φ from the x-axis is given by the following,

$$\mathbf{T}(\Delta, \varphi) = \begin{bmatrix} 1 & 0 \\ 0 & 1 \end{bmatrix} \cos \frac{\Delta}{2} - i \begin{bmatrix} \cos 2\varphi & \sin 2\varphi \\ \sin 2\varphi & -\cos 2\varphi \end{bmatrix} \sin \frac{\Delta}{2}, \quad (1)$$

where $\Delta = 2\pi n_d d / \lambda$, with n_d , d , and λ being the birefringence and thickness of the uniaxial plate, and wavelength of impinging light, respectively. Assuming an incident Jones Vector of $\mathbf{J} = [1 \pm i]^T$,

$$\begin{aligned} \mathbf{J}_{\text{out}}(\Delta, \varphi) &= \mathbf{T}(\Delta, \varphi) \begin{bmatrix} 1 \\ \pm i \end{bmatrix} \\ &= \cos \frac{\Delta}{2} \begin{bmatrix} 1 \\ \pm i \end{bmatrix} + e^{\pm i(2\varphi - \frac{\pi}{2})} \sin \frac{\Delta}{2} \begin{bmatrix} 1 \\ \mp i \end{bmatrix}. \end{aligned} \quad (2)$$

From the equation above, we see that the output Jones Vector contains components that is phase modulated and not modulated, with their relative intensities depending on Δ . When $\Delta = \pi$, the output light only contains light that is phase modulated by twice φ , and inverted in circular polarization sense. Because Δ is in general dispersive, ideal phase modulation only occurs at finite wavelengths. However, this dispersion in phase modulation efficiency can be overcome by using a material with negative wavelength dispersion of birefringence or by stacking two nematic layers twisted in opposite directions [7].

3 PRINCIPLE OF PHASE MODULATION USING PATTERNED CHOLESTERIC LCS

While nematic LCs enable transmissive DOEs to be fabricated, chiral LCs such as cholesteric LCs (ChLCs) enable reflective DOEs, or HOEs to be fabricated [4].

ChLCs are phases in which the constituent LC molecules arrange in a helical fashion. The periodic modulation in the dielectric tensor gives rise to a Bragg reflection band, which reflects light falling in the region $n_o \times p - n_e \times p$, where n_o , n_e and p are the ordinary and extraordinary refractive indices and pitch of the ChLC. When the ChLC is aligned with its helix axis perpendicular to a substrate, the Bragg reflected light acquires a phase that is proportional to twice the orientation angle of the LC on the substrate. Since the orientation of the LC at the substrate defines the structural phase of the helical structure, the orientation angle is also referred to as the helix phase.

In Fig. 1, we numerically simulate the optical properties of a ChLC with varying helix phase. The schematic illustration of the model analyzed by the 4×4 matrix method is shown in Fig. 1(a) [8]. A right-handed ChLC liquid crystal material with extraordinary and ordinary refractive indices $n_e = 1.7$, $n_o = 1.5$, and pitch $p = 700$ nm was modeled, and its reflectance and reflected light phase was calculated as the helix phase was varied from $0 - \pi$ radians. The length of the ChLC was set to $14 \mu\text{m}$ (20 periods).

Figure 1(b-d) shows the magnitude and phase of the reflected and transmitted light for a linearly polarized beam incident on the ChLC. The horizontal axis shows the wavelength, the vertical axis shows the helix phase, and the intensity shows either the reflection magnitude or the phase. Light reflection is observed between $1050 - 1190$ nm, which corresponds to the theoretical reflection band width, $n_o \times p - n_e \times p$. The phase of the Bragg reflected light is found to vary linearly with the helix phase: the phase changes from 0 to 2π by a modulation in helix phase of 0 to π , implying that a full wave control is possible. On the other hand, light that is transmitted experiences no change in phase; this implies that the element can be seen through without any image distortion, regardless of the imprinted pattern.

It is interesting to note the difference in properties between the transmissive DOEs based on uniaxial NLCs and the reflective HOEs based on ChLCs. In NLCs, the incident circularly polarized light changes its circular sense and acquires a phase proportional to 2ϕ ; phase modulation occurs irrespective of the circular polarization, except that the phase gradient is reversed depending on the polarization. For the ChLC, phase modulation only occurs for light that is Bragg reflected from the ChLC. That is, only the circularly polarized component with the same helical handedness as the helix is phase modulated, while the orthogonal polarization is transmitted unaffected.

4 ALIGNMENT DESIGNS FOR SPECIFIC DOE FUNCTIONS

Regardless of their differences, light propagating through both LC-based DOEs and HOEs acquires a phase that is proportional to twice the orientation angle of the LC on the substrate. Thus, the function of the element is

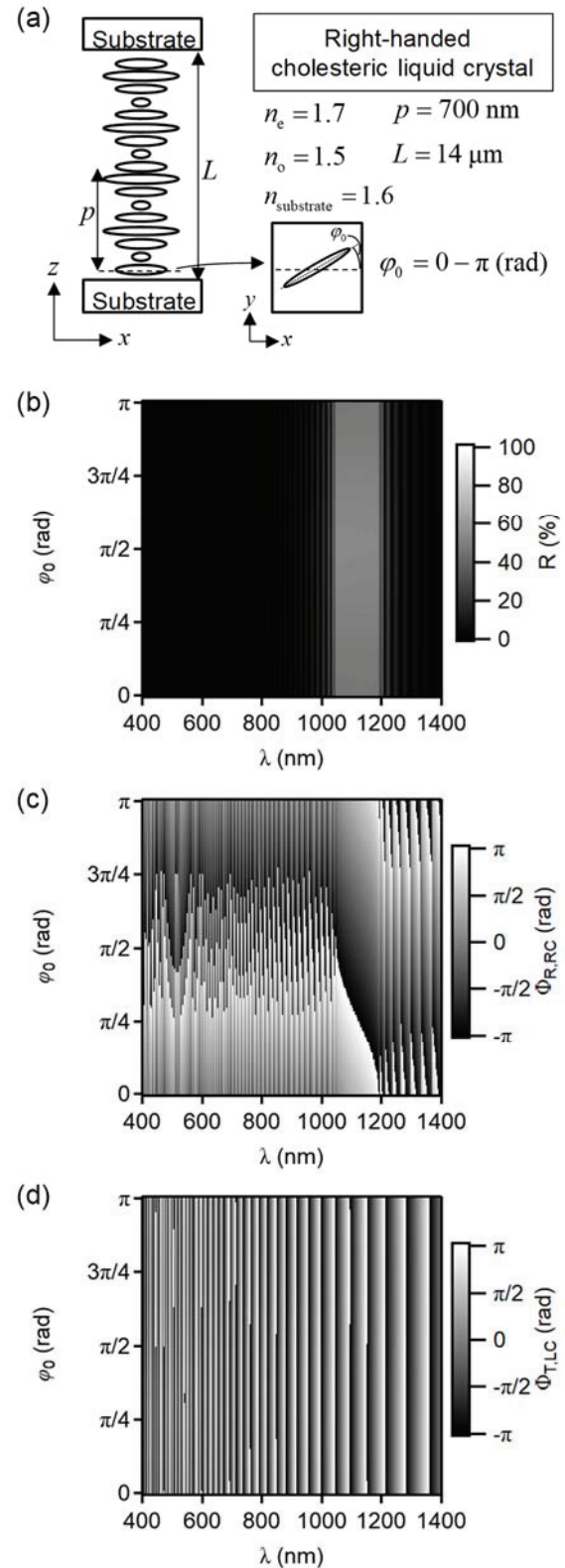


Fig 1. (a) Numerical model of the ChLC. (b) Reflectance for linearly polarized incidence on modelled ChLC. (c) Phase of right-circularly polarized light Bragg reflected from the ChLC. (d) Phase of left-circularly polarized light transmitted through the ChLC.

determined by the alignment design of the LC.

Figure 2(a) shows a streamline illustration of the LC orientation distribution required to achieve a light deflector. A device with a linear modulation in the orientation along a single direction functions as a blazed grating that is capable of deflecting light according to the grating equation:

$$\sin \theta_d - \sin \theta_i = \frac{\lambda}{\Lambda}, \quad (3)$$

where θ_i and θ_d are the incident and diffraction angles, respectively, and Λ is the period over which the LC orientation rotates by π . Several groups have reported the fabrication of fine-pitch gratings that enable diffraction angles above 40° by means of interference exposure [9–11].

A lens element with the capability to focus light can be achieved by creating a distribution that is schematically shown in Fig. 3(b). The orientation angle, and hence optical phase has a parabolic profile: assuming a phase difference of Φ at the center and edge of a lens with a diameter of D , the focal distance of the lens, f , is given by

$$f = \frac{D^2 \pi}{4\Phi \lambda}. \quad (4)$$

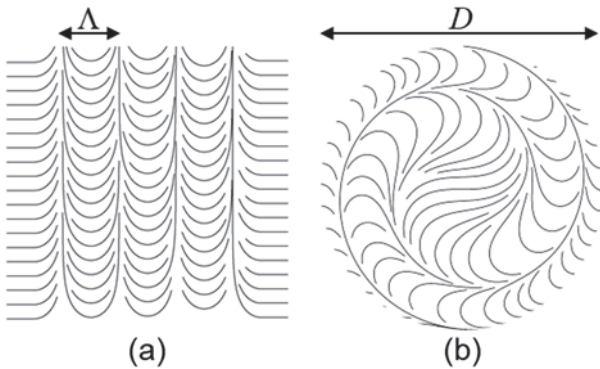


Fig 2. (a) Streamline presentation of LC orientation distribution required to achieve a deflector. (b) LC orientation distribution required for a lens function.

The optical function that can be achieved is not limited to the two devices described above. Because the phase can be modulated by one full wavelength, algorithms for computer-generated holography (CGH) can be employed to numerically design the orientation distribution required to achieve a particular function. Multi-functional beam shaping elements have been demonstrated by designing the orientation with CGH algorithms. [12,13]

5 CHLC-BASED TRANSPARENT HOES

A notable feature of ChLC-based HOEs is that no higher-order reflection is observed for normal incidence, because of the helical modulation of the dielectric tensor (Fig. 1b). This is a unique property not observed in

standard dielectric multilayer devices, where higher-order reflections are unavoidable. This opens new opportunities for LC-based HOEs, since a reflective hologram that appears truly transparent under ambient lighting can be fabricated by appropriate design.

We demonstrated a transparent HOE using a ChLC with a long pitch such that the reflection band appears in the NIR range (1050 – 1200 nm). The ChLC material was filled into a glass sandwich cell with a cell-gap of 9 μm , prepared from a glass substrate treated to have patterned alignment. The classical Gerchberg-Saxton algorithm was employed to numerically obtain the distribution required to reconstruct the Osaka university mascot Dr. Wani illustrated in Fig. 3(a) [14]. The obtained phase distribution is shown in Fig. 3 (b).

The easy axis distribution on the patterned substrate was imprinted using a home-built, maskless photoalignment setup [13]. Fig. 4 shows the appearance and optical spectra of the fabricated ChLC element. Under ambient lighting, the sample appears transparent, despite the Bragg reflection band between approximately 1050 and 1200 nm. The Bragg reflection of dielectric multilayer systems is known to blue-shift with an increase in the angle of light incidence; however, the reflection band does not blue-shift into the visible region regardless of the incidence angle, thus avoiding coloration. The presence of a hologram was confirmed by illuminating an infrared laser on the element and observing the reflected image with an infrared camera. The ChLC element thus has phase information that is concealed in the visible range.

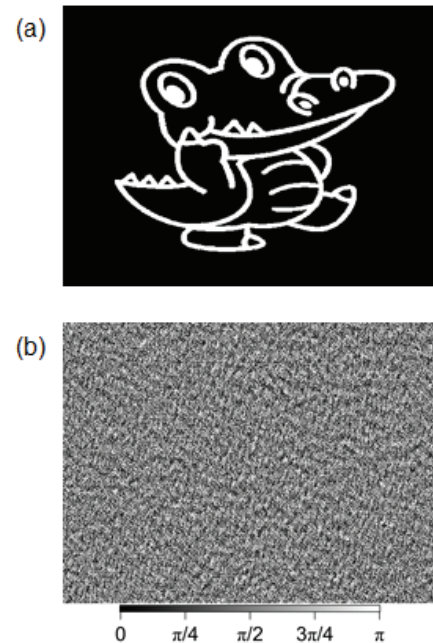


Fig. 1 (a) Target hologram image, the OSAKA UNIVERSITY mascot Dr. Wani. (b) Phase distribution required to generate the image shown in (a).

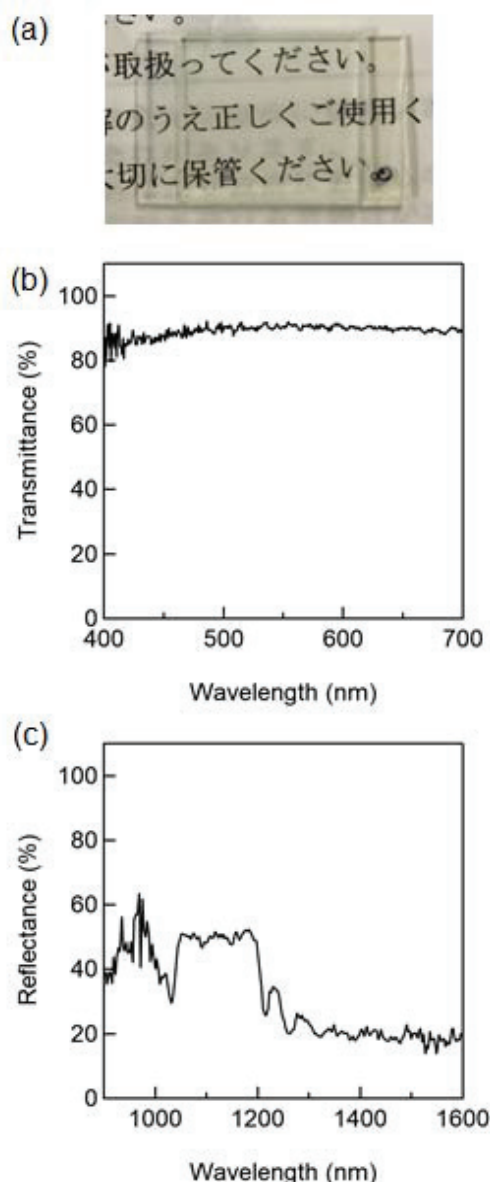


Fig. 2 (a) Appearance of transparent ChLC hologram, (b) Transmittance spectrum of the ChLC in the visible region, (c) Reflectance spectrum of the ChLC in the infrared region.

CONCLUSIONS

The operation principle of DOEs and HOEs based on patterned LCs was reviewed. These optical elements are attractive since tunable devices can be fabricated as well as free standing films by the appropriate choice of LC material. One of the main challenges of the technology is fine-patterning of the LC alignment: however, progress is being made in experimental approaches, such as the use of nanoimprint lithography. With the potential of fabricating large-area devices in a manner similar to LC-based compensation films, these optical elements are promising candidates for use in AR/VR, holographic displays, and signage.

ACKNOWLEDGMENTS

The authors thank DIC Corporation, JSR Corporation, and BASF Japan Corporation for providing materials. This work was partly supported by JST PRESTO (JPMJPR151D), MEXT KAKENHI (17H02766), and Osaka University Innovation Bridge Grant.

REFERENCES

- [1] N. Yu, and F. Capasso, *Nat. Mater.* 13, 139-150 (2014).
- [2] L. Marrucci, C. Manzo, and D. Paparo, *Appl. Phys. Lett.* 88, 221102 (2006).
- [3] N. V. Tabiryan, S. V. Serak, S. R. Nersisyan, D. E. Roberts, B. Y. Zeldovich, D. M. Steeves, and B. R. Kimball, *Opt. Express* 24, 7091-7102 (2016).
- [4] J. Kobashi, H. Yoshida, and M. Ozaki, *Nat. Photon.* 10, 389-392 (2016).
- [5] D. E. Roberts, N. Tabiryan, M. McConney, and T. Bunning, *OSA Imaging and Applied Optics Technical Digest*, paper DM3F.1 (2018).
- [6] Y. Weng, Y. Zhang, J. Cui, A. Liu, Z. Shen, X. Li, and B. Wang, *Opt. Lett.* 43, 5773-5776 (2018).
- [7] C. Oh, and M. J. Escuti, *Opt. Lett.* 33, 2287-2289 (2008).
- [8] D. W. Berreman, *J. Opt. Soc. Am.* 62, 502-510 (1972).
- [9] J. Kobashi, Y. Mohri, H. Yoshida, and M. Ozaki, *Opt. Data Process. Storage* 3, 61-66 (2017).
- [10] X. Xiang, J. Kim, and M. J. Escuti, *Sci. Rep.* 8, 7202 (2018).
- [11] K. Yin, Y. Lee, Z. He, and S. Wu, *Opt. Express* 27, 5814 (2019).
- [12] L. D. Sio, D. E. Roberts, Z. Liao, J. Hwang, N. Tabiryan, D. M. Steeves, and B. R. Kimball, *Appl. Opt.* 57, A118-A121 (2018).
- [13] J. Kobashi, H. Yoshida*, and M. Ozaki, *Sci. Rep.* 7, 16470 (2017).
- [14] R. W. Gerchberg, and W. O. Saxton, *Optik* 35, 237-246 (1972).